IEEE Photonics Journal
An IEEE Photonics Society Publication

Open Access

Phase Sensitive Parametric Process in Silicon Nano-Waveguides at C-Band Wavelengths

Volume 8, Number 5, October 2016

Mahmoud Jazayerifar
Kambiz Jamshidi

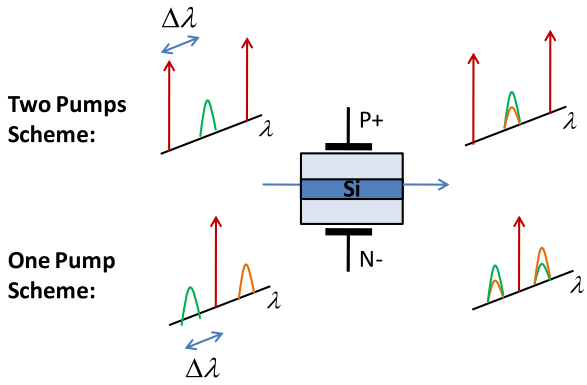

DOI: 10.1109/JPHOT.2016.2603227
1943-0655 © 2016 IEEE

IEEE photonics SOCIETY

IEEE

Phase Sensitive Parametric Process in Silicon Nano-Waveguides at C-Band Wavelengths

Mahmoud Jazayerifar[1] **and Kambiz Jamshidi**[1]

[1]Integrated Photonics Devices Lab., Dresden University of Technology, Dresden 01069, Germany

DOI:10.1109/JPHOT.2016.2603227

Manuscript received June 22, 2016; revised August 19, 2016; accepted August 22, 2016. Date of publication August 30, 2016; date of current version September 14, 2016. This work was supported in part by the German Research Foundation in the context of the "Enhancing Nonlinear Kerr effect in Silicon Nitride Waveguides" project. Corresponding author: M. Jazayerifar (e-mail: mahmoud.jazayeri@tu-dresden.de).

Abstract: Using numerical and analytical tools, we compare different phase sensitive parametric schemes namely one pump and two pump schemes for silicon nano-waveguides. The conditions required to achieve phase sensitive gain are obtained, and it is shown that a real continuous wave phase sensitive parametric gain could be possible in the presence of two photon absorption.

Index Terms: Four wave mixing, silicon nanophotonics, nonlinear integrated optics, nonlinear optical effects in semiconductors.

1. Introduction

Phase sensitive amplifiers (PSA) based on highly nonlinear fibers (HNLFs) have received much interest due to the applications such as low noise amplification and phase regeneration [1], [2]. HNLF-based PSAs have usually a length of few hundreds of meters due to the relatively low optical nonlinear coefficient (∼15 /W/km). In contrasts photonic integrated circuits (PIC) based on glasses or semiconductor material have a larger nonlinear coefficient. For example, due to the high light confinement in silicon nano-waveguides, the nonlinear coefficient in silicon nano-waveguides is larger than 200 /W/m [3], which leads a much smaller footprint (few centimeters) for the same nonlinearity performance [3]. Recently, up to 20 dB of phase sensitive extinction ratio (ER) in silicon nano-waveguides has been reported [3], [4]. One of the main limitations in silicon waveguides is the two photon absorption (TPA) in wavelengths around 1550 nm, which results in the accumulation of free carriers and consequently leads to free carrier absorption (FCA). In order to reduce the FCA, a reversed biased PIN junction can be embedded in silicon waveguides [5] which reduces the FCA significantly. However, the TPA is not reducible by this technique. Because of these nonlinear loss mechanisms in silicon, the four wave mixing (FWM) process in silicon and silica fibers perform differently.

The FWM process in silicon has been widely studied [5]–[9]. Phase sensitive amplifications in silicon waveguides has also been partly investigated before [4], [10], [11]. In [4], silicon PSAs were used for signal regeneration. In [10], phase sensitive amplification has been shown with photonic crystal waveguides. In [11], the noise figure and gain of silicon PSAs have been numerically

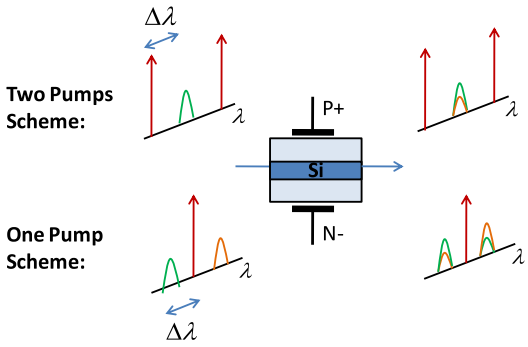

Fig. 1. Schematic explanation of one-pump and two pump PSA with silicon-nanowaveguides.

investigated. In order to achieve a better understanding on the phase sensitive FWM in the presence of TPA and FCA, we have accomplished a comprehensive theoretical study in this paper. We obtain closed form equations for the optimum pump power and detuning, as well as conditions required to achieve FWM phase sensitive gain in silicon, and show that unlike in fibers, the maximum phase sensitive ER and FWM gain are not necessarily achieved together. We compare the two pump and one pump PSA schemes (shown in Fig. 1) and show that unlike in fibers, there are serious differences between these schemes in terms of gain and ER. We also discuss that using a cascaded structure it would be possible to achieve a large parametric gain in silicon nano-waveguides.

2. Modeling

The continuous wave (cw) FWM effect in silicon waveguides can be modeled with the nonlinear Schrödinger equation (NLSE) as follows [9]:

$$\frac{\partial A}{\partial z} + \frac{\alpha_{\text{lin}}}{2}A + \frac{i\beta_2}{2}\frac{\partial^2 A}{\partial^2 t} = i\gamma|A|^2A - \frac{\beta_{\text{TPA}}}{2A_{\text{eff}}}|A|^2A - \frac{\alpha_{\text{FCA}}}{2}A - i\frac{2\pi n_{\text{FCI}}}{\lambda}A \tag{1}$$

where A, α_{lin}, β_2, t, λ, A_{eff}, γ, β_{TPA}, α_{FCA}, and n_{FCI} are the total optical field (including pumps, signal and idler), linear loss, group velocity dispersion parameter, time, optical wavelength, effective area, nonlinear coefficient, TPA coefficient, FCA loss, and free carrier index (FCI) change parameter, respectively, and we have [9]

$$\alpha_{\text{FCA}} = \sigma_{\text{FCA}}N_C,\ n_{\text{FCI}} = \sigma_{\text{FCI}}N_C,\ N_C = \tau\frac{\beta_{\text{TPA}}}{2h\upsilon}\frac{P_P^2}{A_{\text{eff}}^2} \tag{2}$$

where N_C, τ, P_P, υ, σ_{FCA}, and σ_{FCI} are the free carriers density, free carrier life time, total pump power, optical frequency, FCA coefficient, and FCI-related empirical coefficient, respectively [9]. The NLSE can be simulated with the well known split step Fourier method (SSFM). Using SSFM we have investigated a two pump PSA scheme with a pump wavelength separation of 75 GHz which has already been investigated experimentally [4]. We have been able to achieve results similar to the previously reported experimental results [4] which are shown in Fig. 2. This figure shows the difference between the output power and the input power versus the input signal phase for a waveguide with the length of 4 cm. Four pump power levels are considered and the values shown in the figure are before entering the waveguide (after subtracting the grating losses of ~4.5 dB the actual pump power propagating in the waveguide is obtained). In Fig. 2, two extinction ratio values which were measured in [4], are shown which indicates a good agreement between our numerical results and the previously reported experimental results. The simulation results are obtained with the following numerical values:

$$\gamma = 230\ \text{/W/m},\ \beta_{\text{TPA}} = 0.9\times10^{-11}\ \text{m/W},\ D = -2450\ \text{ps/nmkm}$$

$$A_{\text{eff}} = 0.11\ \mu\text{m}^2,\ \alpha_{\text{lin}} = 1.15\ \text{dB/cm},\ \tau = 20\ \text{ps}$$

$$\sigma_{\text{FCA}} = 1.45\times10^{-21}\ m^2\ [9],\ \sigma_{\text{FCI}} = 5.3\times10^{-27}\ \text{m}^3\ [9]$$

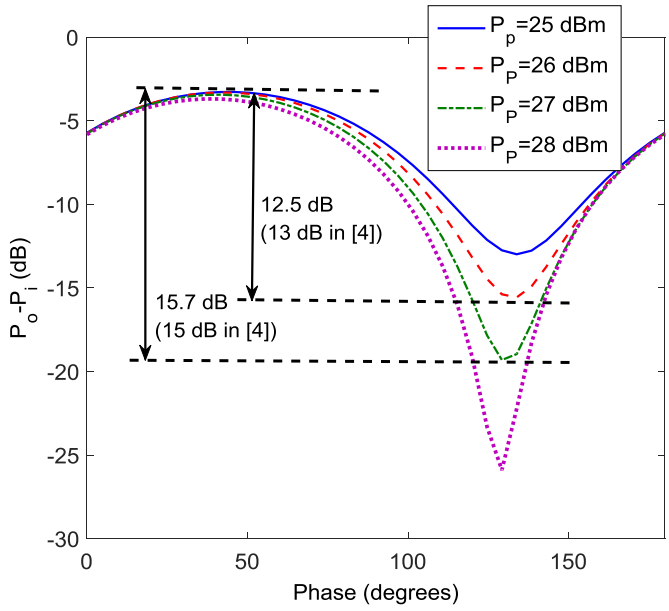

Fig. 2. Output-input signal power difference versus the signal phase for different pump power levels before grating (grating loss = 4.5).

These numerical values will be used in the rest of this paper for both single pump and two pump schemes except in Section 5, where we evaluate gain perspectives with an ideal waveguide.

The signal power is –15 dBm in the rest of the paper. Note that a carrier life time on the order of picoseconds is only achievable with reversed biased PIN junctions which will be used in the rest of the paper.

In Fig. 2 it is observed that the ER increases by increasing the pump power which is an expected effect due to a more intense FWM process at larger pump powers. However, by increasing the pump power the maximum level of the output power decreases which shows that the TPA and FCA losses increase more than the FWM gain at higher pump powers.

In Fig. 3 the output-input signal power difference is shown for different wavelength detuning values in a two pump scheme with a total pump power of 28 dBm before grating (grating loss = 4.5 dB). $\Delta\lambda$ is defined according to Fig. 1. In the two pump scheme, $\Delta\lambda$ is the detuning of the pumps from the center of the two pump wavelengths and in the single pump scheme, $\Delta\lambda$ is the detuning between the pump wavelength and the signal wavelength.

In a two pump scheme, for a specific normal dispersion, there is an optimum detuning which leads to the best phase matching condition and maximum ER [12 App. 5]. However, in Fig. 3 it is observed that the ER reduces as the detuning increases which shows that the optimum detuning level even is lower than 1 nm. At larger pump powers, a larger optimum detuning is expected [12 App. 5]. In Fig. 4 the output-input signal power difference is shown for a larger total pump power (31 dBm before grating). It is observed that a 2 nm detuning seems to be the optimum value in this case. However, applying a pump power of 31 dBm to a nano-waveguide may be difficult in practice.

3. Comparing Two Pump and One Pump Schemes

In Fig. 5, we have compared a two pump scheme with a one pump scheme PSA for the same waveguide and the same total pump power (P_P), i.e. in the two pump scheme, the power of each pump is equal to the half of the pump power of the one pump scheme. It is observed that the output signal power is larger in case of one pump scheme while the ER is larger in the case of two pump scheme. The main reason is that the wavelength separations between pumps is low ($\sim$1 nm) such

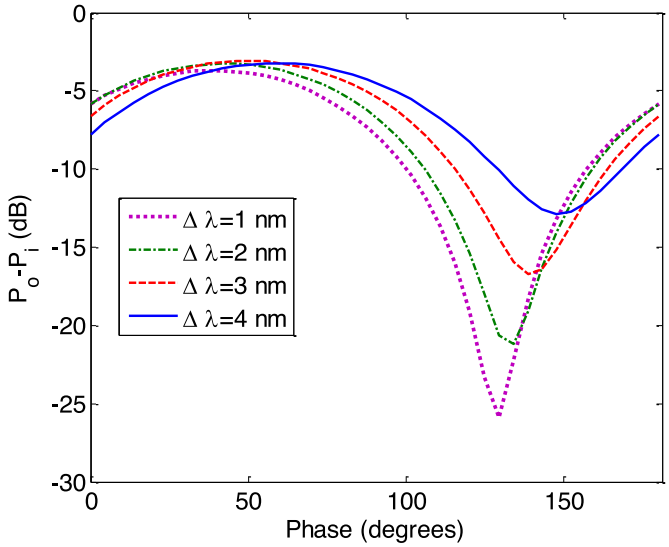

Fig. 3. Impact of different pump wavelength detuning in a two pump scheme with a total pump power of 28 dBm (before grating).

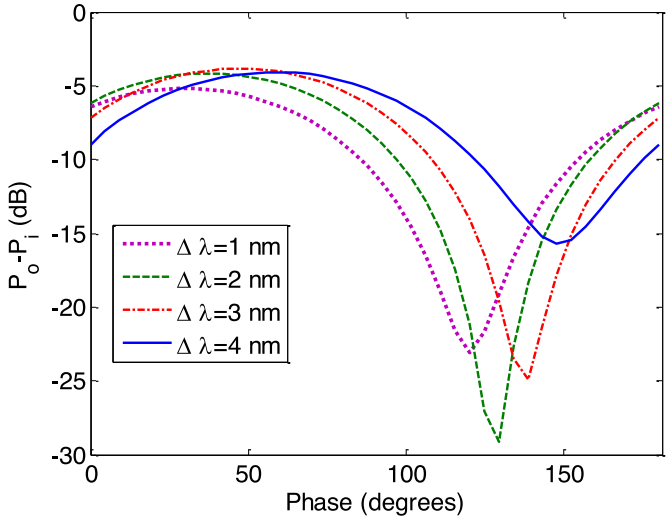

Fig. 4. Impact of different pump wavelength detuning in a two pump scheme with a total pump power of 31 dBm (before grating).

that the walk-off between the pumps while propagation is small and the total pump power in the pump scheme can be approximated as

$$P_P(t) = \left|\sqrt{\frac{P_P}{2}}e^{j\omega_1 t} + \sqrt{\frac{P_P}{2}}e^{j\omega_2 t}\right|^2 = P_P\left(1 + \cos\left((\omega_1 - \omega_2)t\right)\right) \tag{3}$$

where ω_1 and ω_2 are the angular frequencies of the two pumps. From (3), it is clear that $P_P(t)$ can be as large as $2P_P$ at some time instants. Since the nonlinear response is almost instantaneous, this large pump peak power results in a large FWM and TPA. Therefore, for the same average pump power, the two pump scheme experiences more nonlinearity leading to a more TPA loss, as well as a larger ER caused by a more intense FWM.

In Fig. 6, the two pump and one pump schemes are compared with a larger pump power, and it is observed that the one pump scheme leads to a larger ER. Unlike one pump scheme, the ER

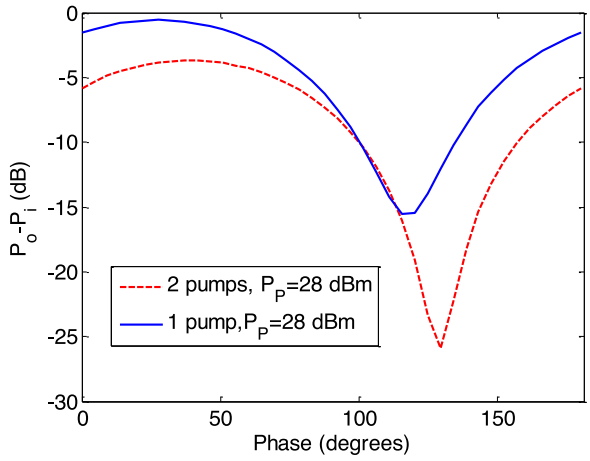

Fig. 5. Comparison of one pump and two pump schemes for the same total pump power of 28 dBm (wavelength detuning is 1 nm).

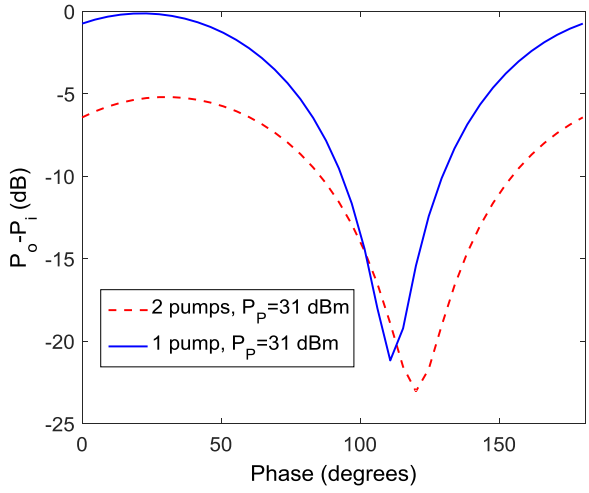

Fig. 6. Comparison of one pump and two pump schemes for the same total pump power of 31 dBm (wavelength detuning is 1 nm).

does not improve in the case of two pump scheme as the pump power increases from 28 dBm to 31 dBm, which is due to the fact that for power levels above a certain threshold, the TPA induced pump depletion becomes so large that it reduces the FWM significantly. Apparently, this threshold is reached at lower average power levels for the two pump case due to the effect explained in (3). From Figs. 4 and 5, it is realized that one pump scheme holds an advantage in terms of gain which is explainable as follows: Considering the tradeoff between FWM and TPA, there is an optimum pump power leading to the maximum gain; however, according to (3), the overall pump power oscillates in a two pump scheme, resulting in deviation from the optimum power during propagation. Note that the problem mentioned with the two pump scheme and (3) can be eliminated if a waveguide with low dispersion is designed such that the pump wavelengths can be adjusted to be far away from each other (similar to the two pump PSAs based on HNLFs [1]).

4. Gain Conditions in a One Pump Scheme

Considering a one pump scheme, here, we discuss the required conditions to achieve phase sensitive gain with silicon nano-waveguides. In addition to the NLSE, the FWM process can be also

modeled via a set of differential equations [13]. Assuming that the pump power is much larger than the signal and idler powers such that the FWM pump depletion is negligible, after including the TPA and FCA losses, the signal, idler, and pump power evolution along the waveguide can be written as

$$\begin{aligned}
\frac{dP_s}{dz} &= 2\gamma P_P\sqrt{P_iP_s}\sin(\theta) - \alpha_{\text{lin}}P_s - \alpha_{\text{FCA}}P_s - 2\frac{\beta_{\text{TPA}}}{A_{\text{eff}}}P_sP_P \\
\frac{dP_i}{dz} &= 2\gamma P_P\sqrt{P_sP_i}\sin(\theta) - \alpha_{\text{lin}}P_i - \alpha_{\text{FCA}}P_i - 2\frac{\beta_{\text{TPA}}}{A_{\text{eff}}}P_iP_P \\
\frac{dP_P}{dz} &= -\alpha_{\text{lin}}P_P - \frac{\beta_{\text{TPA}}}{A_{\text{eff}}}P_P^2 - \alpha_{\text{FCA}}P_P \\
\frac{d\theta}{dz} &\approx \Delta\beta, \quad \Delta\beta = \beta_2(\Delta\omega)^2 + 2\gamma P_P
\end{aligned} \tag{4}$$

where P_i, P_s, P_P, and θ are the idler power, signal power, pump power, and a parameter explaining the phase matching condition [13]. It should be noted that the effect of free carrier index change on the phase matching is not included in (4) because it is negligible compared to the effect of group velocity dispersion for large dispersion values and small wavelength detuning that are considered in the paper. This can be verified from the data which is available in [14].

The initial value of θ is determined by the relative phase of the pump, signal and idler, and for the maximum gain condition it should be equal to $\pi/2$. In order to achieve a positive gain, we should have $dP_s/dz > 0$. Setting $P_s = P_i$ in the above equation (one pump scheme in Fig. 1), after some straight forward algebra, we obtain the following condition:

$$\frac{4\pi}{\lambda}\frac{n_2}{\beta_{\text{TPA}}}\cos(\Delta\beta z) - 2 > \frac{\alpha_{\text{lin}}A_{\text{eff}}}{\beta_{\text{TPA}}}\frac{1}{P_P} + \frac{\sigma_{\text{FCA}}\tau}{2h\upsilon A_{\text{eff}}}P_P \tag{5}$$

where σ_{FCA} is defined in (2), and n_2 is the nonlinear refractive index which is related to the nonlinear coefficient, denoted by γ, through

$$\gamma = \frac{2\pi}{\lambda}\frac{n_2}{A_{\text{eff}}} \tag{6}$$

The right side of (5) can be written as follows:

$$f(P_P) = \frac{a}{P_P} + bP_P, \quad a = \frac{\alpha_{\text{lin}}A_{\text{eff}}}{\beta_{\text{TPA}}}, \quad b = \frac{\sigma_{\text{FCA}}\tau}{2h\upsilon A_{\text{eff}}} \tag{7}$$

where $f(P_P)$ has a minimum with respect to P_P. By solving the equation $\partial f(P_P)/\partial P_P = 0$, the pump power which minimizes $f(P_P)$ is obtained to be $P_P = (a/b)^{1/2}$ which leads to the following equation for the optimum pump power:

$$P_{P,\text{Opt}} = A_{\text{eff}}\sqrt{\frac{2\alpha_{\text{lin}}h\upsilon}{\sigma_{\text{FCA}}\tau\beta_{\text{TPA}}}}, \tag{8}$$

This value of pump power is the power in which dP_s/dz is maximized, and the FWM gain has its maximum level. Therefore, we call it optimum pump power and denote it by $P_{P,\text{Opt}}$. Note that as the pump propagates in the waveguide, it is depleted mostly by TPA and FCA such that only over a limited propagation length the pump power can be close to the optimum value.

We can also calculate the optimum dispersion level (at a certain detuning). In the perfect phase matching condition, $\Delta\beta = 0$, which (according to (4)) leads to

$$D_{\text{Opt}} = \frac{2n_2\lambda}{c(\Delta\lambda)^2}\frac{P_P}{A_{\text{eff}}} \tag{9}$$

where D_{Opt} is the optimum dispersion value for a pump-signal detuning of $\Delta\lambda$. Note that the optimum dispersion is anomalous in the case of one pump scheme while it is normal in the case of two pump scheme [12 App. 5].

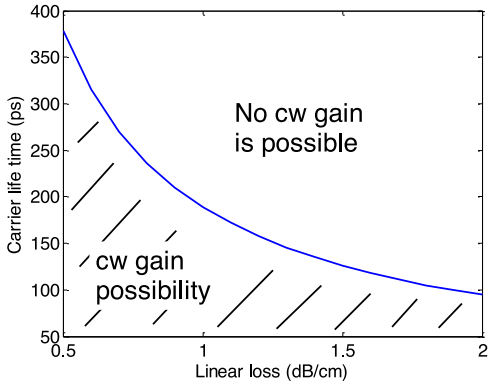

Fig. 7. Carrier life-time and linear loss values for which the gain could be achievable according to the necessary (no sufficient) condition (see (10)).

We can also obtain a general gain condition for a waveguide as follows. At the best condition we have the optimum pump power which was obtained in (8) and the dispersion has its optimum level which leads to the perfect phase matching condition, i.e., $\Delta\beta = 0$. Consider equation (5). By inserting the optimum pump power (see $P_{P,\mathrm{Opt}}$ in (8)) into $P_{P,}$ and letting $\Delta\beta = 0$, the (5) simplifies to the following inequality:

Gain Condition:

$$\frac{4\pi}{\lambda}\frac{n_2}{\beta_{\mathrm{TPA}}} - 2 > \sqrt{\frac{2\alpha_{\mathrm{lin}}\sigma_{\mathrm{FCA}}\tau}{\beta_{\mathrm{TPA}}h\upsilon}} \tag{10}$$

which serves as a general necessary condition to achieve parametric gain in any material with TPA. Note that it is not a necessary condition, and it provides a kind of upper bound for the gain condition since it is based on having perfect phase matching and optimum pump power along the waveguide. However, if (10) is not satisfied no gain will be possible. In Fig. 7, we have shown the carrier life time and linear losses values which satisfy (10). It turns out that (10) leads to a relatively wide upper band for the gain condition. The main reason is the significant pump depletion along the waveguide which limits the gain in two ways: Firstly the pump depletion results in the deviation of the propagating pump power from the optimum pump level value which leads to the reduction of the gain. Secondly as the pump is depleted the pump induced nonlinear phase shift changes such that the perfect phase matching condition will be no longer satisfied. Note that in the perfect phase matching condition we have $\Delta\beta = 0$, which is due to a balance between dispersion-induced and nonlinear-induced phase shifts, and it can only be satisfied over a long waveguide if the pump power is relatively constant while propagation (which leads to a constant nonlinear phase shift).

Assuming that the input phases are such that the FWM has its maximum phase sensitive gain at the input of the waveguide, we have numerically obtained the distance over which, the FWM is still larger than the total losses. We call this distance gain length, which is shown in Fig. 8. Fig. 8 is obtained from (4). The numerical values used in the figure are mentioned in Section 2. In Fig. 8, the full green line shows the case of a small pump-signal wavelength detuning ($\Delta\lambda = 1$ nm), where both pump depletion and FWM phase mismatch are taken into account. Fig. 8 can be explained through (5). The pump depletion not only changes the right side of (5) but reduces the left side by changing the phase matching term *($\Delta\beta$)* as well. This shows that the gain length is not only limited by the pump depletion itself but also by the phase mismatch which is induced by the pump depletion.

The dotted blue line shows the maximum theoretical limit with the perfect phase matching condition over the whole propagation length. In other words, we have assumed that $\Delta\beta = 0$ in (5) for the dotted blue line. Therefore, the left-side of (5) is constant, and the pump depletion only changes

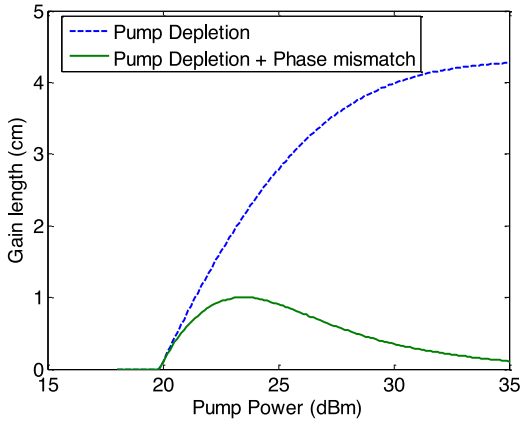

Fig. 8. Length over which the FWM gain overcomes the losses versus pump power for a 1 nm detuning (full green line) (Dotted blue line) Theoretical, limit assuming perfect phase matching along the whole waveguide.

the right side of (5). The dotted blue line shows the gain length which is only limited by the pump depletion without considering the corresponding phase mismatch. From Fig. 8, it is realized that the length over which gain is achievable and is limited, and in order to obtain a positive gain, a limited length should be used.

5. Perspectives of Gain in a One Pump Scheme

As explained in Section 4, the gain is limited by the pump depletion and its impact on the phase matching condition. In order to overcome these limitations, we can consider a multi-stage cascaded scheme in which the pump can be injected at several points along the waveguide to compensate for the pump depletion and the pump phase at each stage can also be adjusted such that a relative phase of $\pi/2$ for the maximum gain is restored. In this way a phase sensitive gain at each stage is achieved and after several stages a large gain could be achieved. In order to achieve a prospective of the achievable gain level, here we consider an optimum waveguide design which may be difficult to implement with the current technology. We assume the following dispersion and loss values:

$$D = 1500 \text{ ps/nmkm}, \ \alpha_{\text{lin}} = 0.5 \text{ dB/cm}.$$

We assume a grating loss of 3 dB, and an input pump power of (28.5 dBm) before grating. Using these values the optimum detuning and length (per stage) is estimated by our SSFM simulations to be around 8 nm and 5 cm, respectively. Using these values, we have simulated the achievable gain shown in Fig 9, which shows the gain at the end of each stage, and we assume the same pump power and the same FWM relative phase at the input of each stage. From Fig. 9, it is realized that using a cascaded structure, an on-off cw phase sensitive gain of up to 20 dB could be feasible with silicon nano-waveguides, despite the nonlinear loss mechanism in silicon.

6. Conclusion

We have shown that for the same total pump power, the two pump PSA scheme leads to a larger ER compared to the one pump PSA scheme due to the beating between pumps and its impact on FWM. However, the one pump scheme performs better in terms of gain because there is no pump beating effect, and the pump power can be adjusted to be close to the optimum level. We have obtained closed form equations for the optimum pump power and the optimum dispersion level as well as a closed form equation serving as a necessary condition for having parametric gain in the presence of TPA and FCA. It was shown that the distance over which the parametric gain is

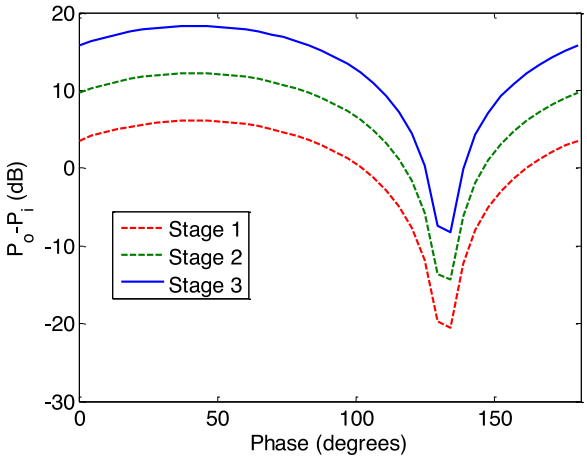

Fig. 9. Phase-sensitive gain at the end of stage 1 to stage 2 for an input pump power of 28.5 dBm (before a grating with 3 dB loss). Optimum waveguide with anomalous dispersion and a linear loss of 0.5 dB/cm.

achievable is limited due to the pump depletion and its impact on the phase matching condition. We discussed that by using a cascaded structure, it is possible to compensate for the pump depletion effect. In this way, the distance over which a positive parametric gain is achievable is extended, which makes it possible to achieve a large gain in silicon nano-waveguides with reversed bias PIN junctions despite the degrading effect of nonlinear loss mechanisms.

Acknowledgment

The authors would like to thank Prof. K. Petermann and Dr. L. Zimmermann for their constructive remarks and suggestions.

References

[1] M. Marhic, S. Radic, C. Peucheret, P. Andrekson, and M. Jazayerifar, "Fiber optical parametric amplifiers for optical communication," *Laser Photon. Rev.*, vol. 9, no. 1, pp. 50–74, 2015.
[2] Z. Tong *et al.*, "Towards ultrasensitive optical links enabled by low-noise phase-sensitive amplifiers," *Nature Photon.*, vol. 5, pp. 430–436, 2011.
[3] K. Petermann *et al.*, "Phase-sensitive optical processing in silicon waveguide," presented at the Opt. Fiber Commun. Conf., 2015, Paper Tu2F.4.
[4] F. Da Ros *et al.*, "Phase regeneration of DPSK signals in a silicon waveguide with reverse-biased pin junction," *Opt. Exp.*, vol. 22, no. 5, pp. 5029–5036, 2014.
[5] A. Gajda *et al.*, "Highly efficient cw parametric conversion at 1550 nm in SOI waveguides by reverse biased P-I-N junction," *Opt. Exp.*, vol. 20, no. 12, pp. 13100–13107, 2012.
[6] H. Fukuda *et al.*, "Four-wave mixing in silicon wire waveguides," *Opt. Exp.*, vol. 13, no. 12, pp. 4629–4637, 2005.
[7] M. A. Foster, A. C. Turner, R. Salem, M. Lipson, and A. L. Gaeta, "Broad-band continuous-wave parametric wavelength conversion in silicon nanowaveguides," *Opt. Exp.*, vol. 15, no. 20, pp. 12949–12958, 2007.
[8] R. M. Osgood *et al.*, "Engineering nonlinearities in nanoscale optical systems: Physiscs and applications in dispersion-engineered silicon nanophotonic wires," *Adv. Opt. Photon.*, vol. 1, no. 1, pp. 162–235, 2009.
[9] I. D. Rukhlenko, M. Premaratne, and G. P. Agrawal "Nonlinear silicon photonics: Analytical tools," *IEEE J. Sel. Topics Quantum Electron.*, vol. 16, no. 1, pp. 200–214, Jan./Feb. 2010.
[10] Y. Zhang *et al.*, "Phase-sensitive amplification in silicon photonic crystal waveguides," *Opt. Lett.*, vol. 39, no. 2, pp. 363–366, 2014.
[11] W. Li and X. Sang, "Phase-sensitive parametric amplifiers in silicon waveguides," *J. Modern Opt.*, vol. 58, no. 14, pp. 1246–1251, 2011.
[12] M. E. Marhic, *Fiber Optical Parametric Amplifiers, Oscillators and Related Devices*, 1st ed. Cambridge, U.K.: Cambridge Univ. Press, 2008, p. 146.
[13] G. Cappellini and S. Trillp, "Third order three-wave mixing in single-mode fibers: Exact solutions and spatial instability effects," *J. Opt. Soc. Amer. B*, vol. 8, pp. 824–838, 1991.
[14] N. Milos, R. Soref, and G. Z. Mashanovich, "Free-carrier electrorefraction and electroabsorption modulation predictions for silicon over the 1–14-infrared wavelength range," *IEEE Photon. J.* vol. 3, no. 6, pp. 1171–1180, Dec. 2011.